Behaviour of Mean and Oscillating $E \times B$ Plasma Flows and Turbulence Interactions during Confinement Mode Transitions

G.D. Conway[1], C. Angioni[1], E. Poli[1], F. Ryter[1], P. Sauter[1], B. Scott[1], T. Happel[2], J. Vicente[3] and the ASDEX Upgrade Team

[1]Max-Planck-Institut für Plasmaphysik, EURATOM Association, D-85748 Garching, Germany
[2]Laboratorio Nacional de Fusión, Euratom-Association CIEMAT, 8040, Madrid, Spain
[3]Instituto de Plasmas e Fusão Nuclear, Associação Euratom-IST, 1049-001, Lisboa, Portugal

e-mail contact of main author: Garrard.Conway@ipp.mpg.de

Abstract. The interaction of geodesic acoustic modes (GAMs - turbulence driven $E \times B$ oscillating zonal flows), mean equilibrium flows and the edge turbulence is investigated across the L-H transition in the ASDEX Upgrade tokamak using high resolution Doppler reflectometry. Approaching the transition at low edge plasma collisionalities $\nu^*_{edge} \sim 1$, a few kHz limit-cycle oscillation/pulsing forms, driven by the turbulence and suppressed by the GAM flow shear. With increasing heating power the GAM shearing strengthens (larger amplitude, narrower width) and the pulse length decreases. Eventually the mean equilibrium flow shear starts to dominate, suppressing the pulsing & GAM, which is replaced by large amplitude broadband flow perturbations. At higher densities the limit-cycle action is diminished.

1. Introduction

In magnetic confinement devices, such as tokamaks, turbulence driven $E \times B$ plasma zonal flows (ZFs) and geodesic acoustic modes (GAMs) play an important role in regulating turbulent transport, by enhancing the velocity shearing of turbulent eddies and by providing an additional energy sink through collisional and/or Landau damping (cf. [1–3] and references therein). Turbulence suppression by flow shearing is usually associated with the large (radial) scale mean equilibrium driven $E_r \times B$ flows (i.e. pressure gradient and poloidal and toroidal plasma rotation) [4]; and in the high gradient, high rotation edge region of the high confinement H-mode this is believed to be the dominant factor. However, in the low confinement L-mode regime the mean equilibrium flows are generally weak so that the localized edge GAM (a few kHz coherent flow oscillation which replaces the more core localized zero-mean-frequency ZF) provides the dominant turbulence shearing effect. The crucial question is what happens during L-H confinement transition and what role ZFs play in triggering the transport barrier formation. ZF models, such as the predator-prey model of Kim and Diamond [5], which include mean equilibrium $\langle v_{E\times B} \rangle$ flows, oscillatory $\tilde{v}_{E\times B}$ ZFs and the turbulence, indicate a complex interaction of the three players, particularly when close to mode transitions. There is much experimental evidence to support this model, such as increased turbulence driven Reynolds stress and low frequency flows in the edge shear region prior to and during L-H transitions [6,7]. The impact of the mean flow shear on the ZF/GAM spectrum has also been noted in recent (toroidal) torque scans performed on DIII-D [8], as well as the fact that the GAM, which is universally observed in ohmic and additionally heated L-mode regimes, remains suppressed in the H-mode [9], even when the edge turbulence level recovers later in H-mode due to steepening edge gradients - i.e. the interaction of the flows is as important as the turbulence level.

In this paper we report recent measurements of GAM and edge turbulence behaviour across the L-H transition in the ASDEX Upgrade tokamak using microwave Doppler reflectometry to directly measure the $E_r \times B$ flow and its fluctuations with high spatial (few mm radially) and temporal (sub microsecond) resolution. A clear turbulence-flow interaction is observed close to the L-H threshold at low plasma collisionality with the onset of sustained limit cycle oscillations involving the GAM intensity, mean flow and turbulence.

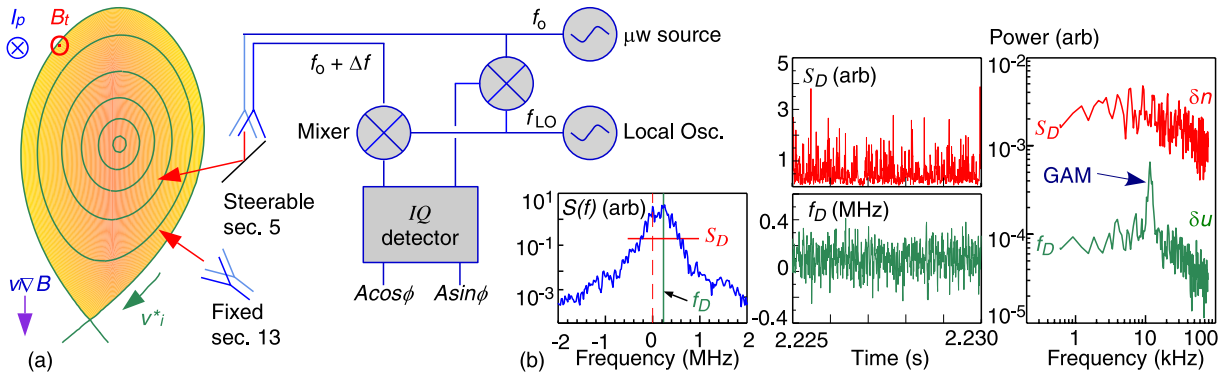

FIG. 1: (a) Schematic of AUG Doppler reflectometers and (b) GAM measurement procedure.

2. Doppler reflectometry measurement technique

Doppler reflectometry is a hybrid diagnostic technique combining the turbulence wavenumber selectivity of coherent scattering with the radial localization of microwave reflectometry. The transceiver antennae are tilted obliquely to the plasma surface (in the plane perpendicular to the magnetic field) to make the diagnostic sensitive to density fluctuation wavenumbers satisfying the Bragg backscatter condition $k_\perp = -2k_o N_\perp$, where k_o is the probing wavenumber and $N_\perp$ the plasma refractive index (perpendicular component) at the reflection layer (obtained via ray/beam-tracing). The fluctuation spectrum of the backscattered signal $S(f)$ is Doppler frequency shifted $f_D = u_\perp k_\perp / 2\pi$ proportional to the fluctuation velocity $u_\perp = v_{Er\times B} + v_{ph}$ (i.e. plasma $E_r \times B$ plus turbulence phase velocities). Generally $v_{Er\times B} \gg v_{ph}$ so that $E_r = 2\pi f_D B / k_\perp$. Hence, fluctuations in the radial electric field E_r appear directly in the Doppler shift [9]. For the results reported here, two $50-75$ GHz tunable frequency channels operated in X-mode were used [10], located in toroidal sectors 5 and 13, $\Delta\phi \sim 180°$ apart and probing lines of sight from the low-field-side, $\Delta\theta \sim 30°$ poloidally apart. *FIG. 1(a)* shows schematically one system and the antennae positions on ASDEX Upgrade (AUG). Sliding an FFT window through the 20 MHz sampled in-phase and quadrature signals, *FIG. 1(b)*, generates time sequences of the mean $f_D = \sum f.S(f) / \sum S(f)$ and spectral intensity $S_D = \sum S(f) \propto |\tilde{n}(k_\perp)|^2$ [9].

3. The L-H transition at low plasma density

GAMs are more clearly observed in the plasma edge at lower densities and higher safety factors q [11] due to weaker collisional and Landau damping [1]. Hence the L-H transition is preferentially studied in low density $\bar{n}_{eo} < 4 \times 10^{19}$ m^{-3} discharges with high $T_{eo} \sim 5$ keV using electron cyclotron resonance (ECR) heating. In this low collisionallity regime, $\nu^*_{edge} \propto n_e / T_e^2 \sim 1$, the transition from L-mode to H-mode in AUG is not direct but proceeds through an intermediate state (labeled I-phase). This state, which is not transitory but can be maintained for many seconds, or indeed the entire discharge length, retains many L-mode features, such as the absence of a pronounced edge temperature pedestal and no apparent ELM ac-

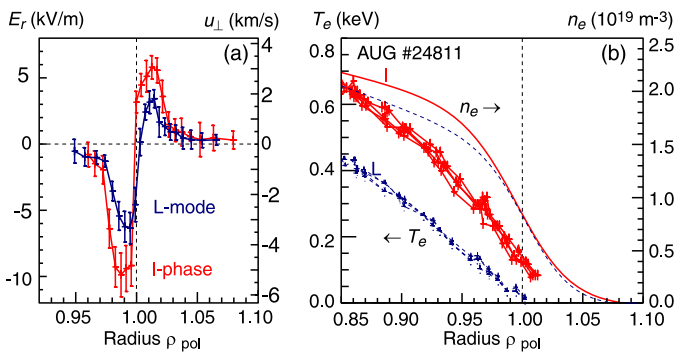

FIG. 2: Edge profiles of (a) E_r & $u_\perp$, (b) n_e and T_e for typical L-mode (blue) and I-phase (red) #24811.

tivity in the usual D_α emission signals, but has an improved energy confinement (approaching weak H-mode values) with a deeper edge negative E_r well (e.g. mean $E \times B$ flow velocity) typically a factor of 2 deeper than the preceding L-mode. *FIG. 2* shows edge profiles of (a) mean E_r, e.g. $u_\perp$ flow, and (b) density (FMCW reflectometer) & electron temperature T_e (ECE) for a typical ECR heated discharge with L-mode (0.35 MW) and I-phases (1.1 MW). In this case there is a steepening of the edge T_e gradient but no clear pedestal formation. Note also the inward movement of the E_r well (minimum) position with the consequent steepening of both positive and negative E_r shear regions in the intermediate phase. This E_r well movement is very typical with improving confinement in L as well as H-mode conditions.

Using a combination of ECRH and neutral beam injection (NBI) power ramping a gradual transition from the L-mode to the H-mode can be engineered. An example is shown in *FIG. 3* with time traces of edge n_e, T_e, D_α, the energy confinement factor $H_{98y2} = \tau_E/\tau_{Escale}$ and outer divertor tile shunt current I_{div} for a $B_T = -2.3$ T, $I_p = 1.0$ MA, $q_{95} \sim 4$, $\bar{n}_{eo} = 2.8 \times 10^{19}$ m^{-3}, $T_{eo} \sim 5$ keV, lower single-null discharge #24750 with a favorable ∇B X-point direction. The power waveforms show the NBI heating ramped from 0 to 1.4 MW with 1.4 MW additional ECRH. Towards the end of the density ramp-up at around 1.65 s the shunt current begins to pulse and the D_α signal rolls-over (I-phase) indicating a drop in particle recycling. Around 2.35 s, the D_α drops slightly, and the pulsing diminishes and an edge T_e pedestal forms (H-mode). H_{98} and (mean) E_r minimum rise from 0.6 and -5.5 kV/m (L) to 0.7 and -8.9 kV/m (I) to 0.8 and -24.5 kV/m in the H-mode respectively. Above the time-traces are time-resolved Doppler reflectometer spectrograms $S(f,t)$ and time-averaged f_D & S_D spectra for the three phases which illustrate the change in the edge turbulence behaviour just inside the E_r minimum radius at $\rho_{pol} = 0.988$ (normalized poloidal flux radius).

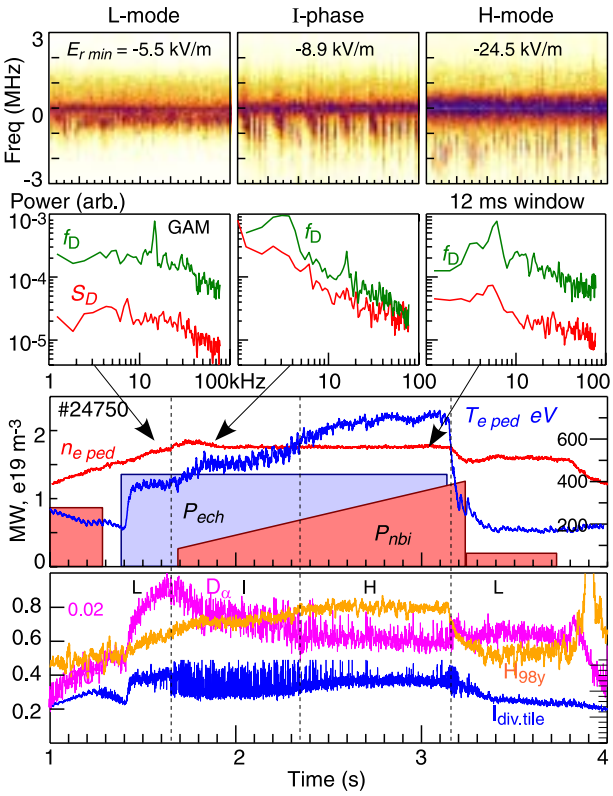

FIG. 3: Top: Time resolved Doppler spectrograms $S(f,t)$ and time averaged f_D & S_D spectra from around E_r minimum at $\rho_{pol} = 0.988$ for L, I and H-mode phases. Lower: corresponding plasma parameter time traces/waveforms for #24750.

4. Edge turbulence & GAM behaviour

In the pure L-mode the edge density fluctuations are broadband, extending up to several hundred kHz, decreasing in amplitude towards the core. The f_D (i.e. $\tilde{E}_r$) and $S_D(k_\perp \sim 10\ \text{cm}^{-1})$ spectra are somewhat flatter than the usual low $k \sim 1$ cm^{-1} density spectrum, with a high-frequency spectral index closer to unity. A coherent GAM peak around 14 kHz is clearly visible in the f_D spectrum, however, there is no evidence of any low frequency ZF activity, either a peak or broadening of the spectra around zero frequency. The spectra continues to be flat down to the lowest spectral resolution investigated (a few tens of Hz). The turbulence is generally continuous, as shown in the time resolved spectrogram $S(f,t)$.

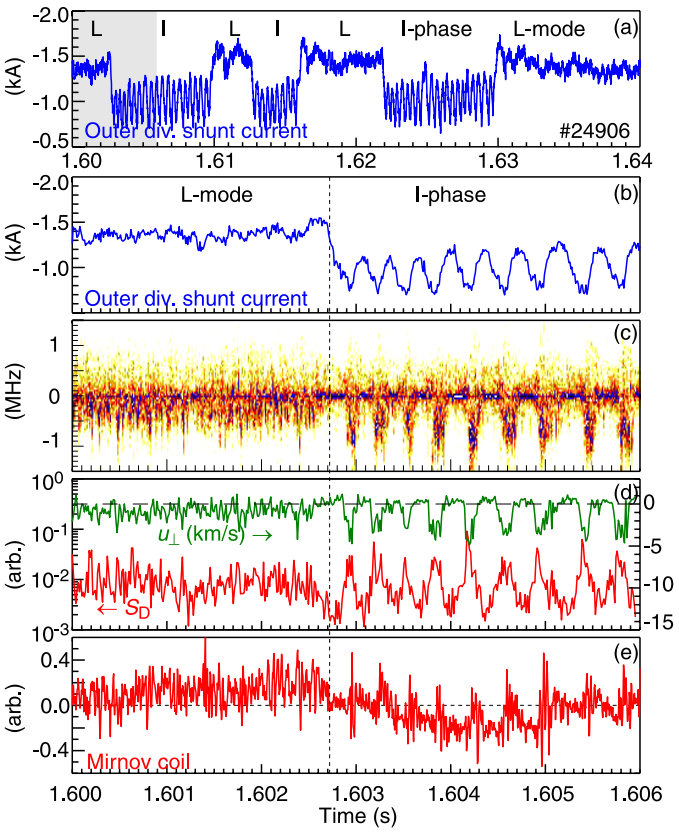

FIG. 4: (a) Divertor tile current with (b) expanded time range, (c) Doppler spectrogram, (d) $u_\perp$ flow velocity & S_D fluctuation power (e) magnetic signal for L & I phases of #24906.

From the low density L-mode raising either the heating power or the density leads to a sharp transition to the I-phase. The turbulence rises across the entire edge region and begins to pulsate at around $2-4$ kHz (sometimes with a slower sub-pulse activity of a few hundred Hz) with an on-off duty cycle of $< 50\%$, as shown in the spectrograms of *FIG. 3* and *FIG. 4(c)*. The kHz pulsing is also observed in the scrape-off-layer (SOL) T_e / flow (divertor tile shunt currents), edge magnetic pick-up coils, plasma loop voltage, and sometimes in edge T_e ECE channels. *FIG. 4* shows an example close to the density/power threshold from a $q_{95} \sim 4$, 2.8×10^{19} m^{-3}, 3.5 keV discharge, #24906, with 1 MW ECRH which exhibits several longer scale dithers between L and I phases. The expanded traces below show more clearly the behaviour over a single transition. The Doppler spectrogram (close to the E_r minimum) together with the corresponding (smoothed) $u_\perp$ velocity and S_D fluctuation power, *FIG. 4(c) & (d)*, show the strong modulation of the E_r well depth, synchronized with turbulence variations between an enhanced and a reduced fluctuation state.

The GAM is still present in the I-phase, however, only clearly during the enhanced turbulence state. *FIG. 5* shows the instantaneous Doppler frequency $f_D = d\phi/dt$ (50 ns resolution) time-

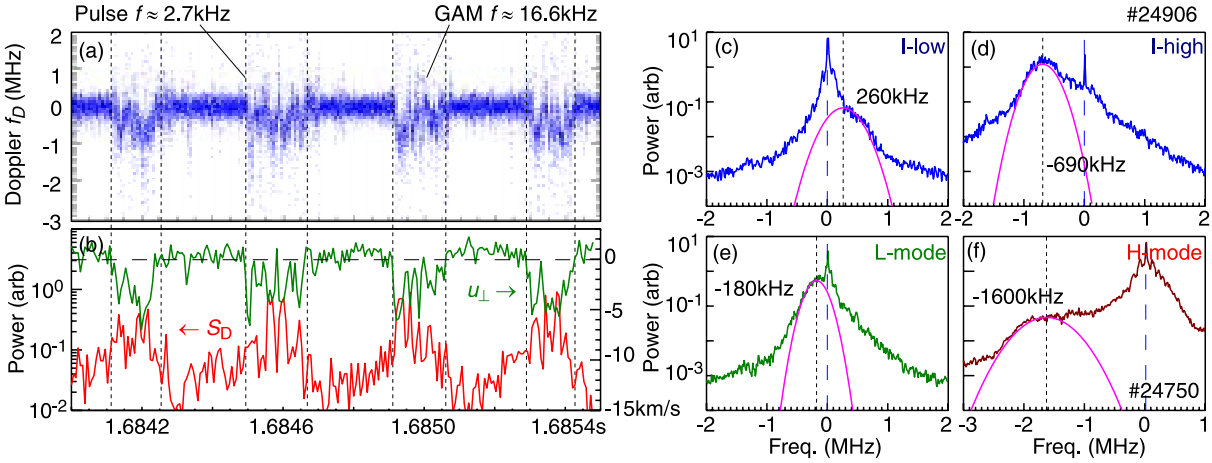

FIG. 5: (a) f_D plus (b) $u_\perp$ & S_D time traces over several I-phase pulses showing strong GAM oscillation, plus synchronized Doppler spectra from (c) low and (d) high I-phases, (e) L-mode earlier in same #24906 and (f) H-mode from similar discharge #24570.

trace from later in the discharge which encompasses several I-phase pulses with an approximately 2.7 kHz repetition. Also shown are "box-car" averaged Doppler spectra $S(f)$ synchronized to the pulse phases, together with a pure L-mode spectrum, and an H-mode spectrum from discharge #24570 for comparison. The strength of the Doppler peak is proportional to the turbulence level. Between the pulses the edge turbulence level first rises, reaches a threshold, then jumps, triggering a fast switching (in < 1 μs, i.e. turbulence time scale) to an enhanced mean E_r well depth and the onset of a very large GAM oscillation (around 16.6 kHz) which is clearly observable in the raw f_D signal. The peak-to-peak GAM amplitude is in-excess of 100% of the mean flow - stronger than in the L-mode prior to the onset of the pulsing. The corresponding E_r shearing rate due to both the pulsing and the GAM oscillation well exceeds the turbulence decorrelation rate. This strong flow shearing action almost immediately begins to reduce the turbulence, and on reaching the threshold (some hysteresis is possible) the flow and GAM switch off. In this case the mean flow even reverses to become positive. Similar flow reversals were recently observed using gas-puff imaging on NSTX just prior to the L-H transition [13] and post L-H dithering has also been noted in TJ-II [12] with a similar behaviour.

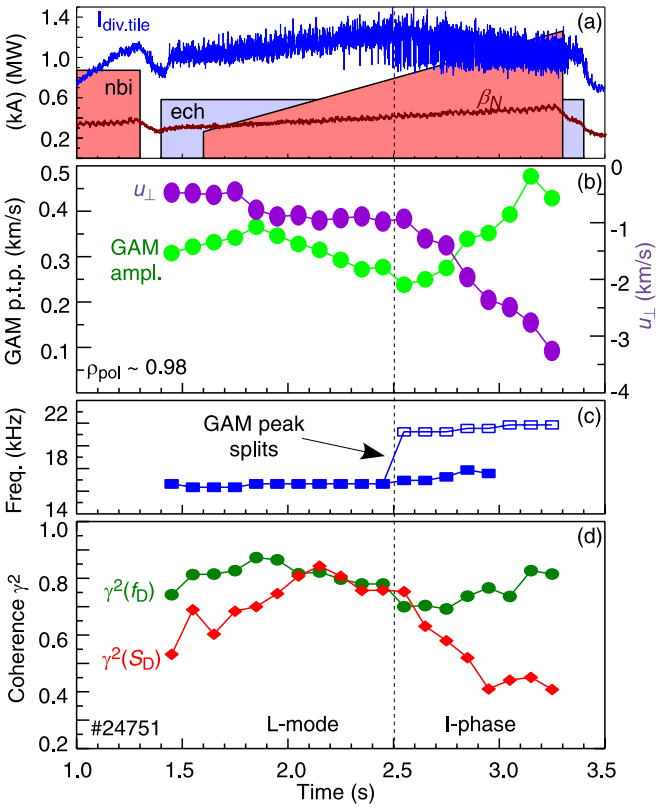

FIG. 6: Evolution of GAM amplitude and mean $E \times B$ velocity across L to I-phase, plus long range (toroidal) coherence γ^2 of GAM f_D and S_D peaks.

The pulse frequency is generally less than a quarter of the GAM frequency so at best only 2 to 3 GAM periods are visible. There are also indications that pulse period decreases with increasing GAM amplitude. All these observations, particularly the GAM onset threshold - also previously noted for the turbulence drive (temperature gradient) [11] - are the the features of a limit cycle behaviour.

FIG. 6 is a good illustration of the link between the GAM behaviour (oscillating $E \times B$ flow) and the mean equilibrium driven $E \times B$ flow. With increasing input power the GAM frequency rises gently with the increasing edge temperature, but bifurcates with the onset of the I-phase pulsing. The edge $u_\perp = v_{E\times B}$ velocity begins to spin-up and the (100 ms time-averaged) GAM peak-to-peak amplitude changes from decreasing (with continuous turbulence level) to increasing (with 50% turbulence modulation). Finally, the mean flow shear begins to dominate over the GAM shearing and the GAM amplitude starts to fall.

5. Transition to H-mode

Returning to discharge #24750 shown in *FIG. 3*, with increasing power a point is reached around 2.35 s where the pulsing begins to diminish, the D_α emission drops slightly and a clear, but weak ELM-free, H-mode T_e pedestal forms. The E_r well depth increases significantly, indicating a mean flow shear dominant regime. At this point the GAM oscillation is no longer observed anywhere in the edge region. There is also a qualitative change in the turbulence behaviour. The

RMS density turbulence level drops across the pedestal region and the turbulence becomes more intermittent with short, semi-random pulses. In the example shown in *FIG. 3* the intermittency frequency rises up to $5.5 - 6$ kHz and the duty cycle drops to less than 30%. Essentially the turbulence pulse becomes too short to sustain a complete GAM period. Overall, the GAM disappears into a rising level of background broadband flow fluctuations, i.e. the $E_r \times B$ flow spectral power moves out of the coherent GAM into large amplitude random flow fluctuations, as shown in *FIG. 3*. Estrada has reported a similar increase in the low frequency flow fluctuations in the H-mode in the TJ-II stellarator [14]. *FIG. 7* shows the evolution of the time-averaged p.t.p GAM amplitude radial profile for #24750. The GAM initially extends zonally some 2 cm from inside the separatrix with a clear maxima in the L-mode phase towards the top of the density pedestal. The arrows indicate the position of the E_r well at the various times. As the confinement improves in the I-phase the GAM zonal extent is eroded from the outer edge, commensurate with radial inward movement of the E_r well minima - i.e. the GAM is only clearly observed in the negative E_r shear region. This again highlights the linkage between the mean and oscillating flows.

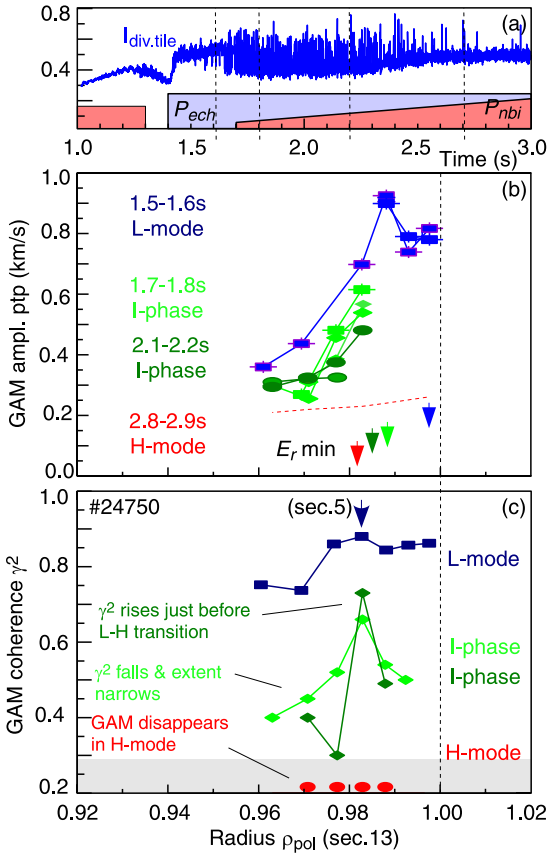

FIG. 7: Radial profiles of GAM p.t.p amplitude (b) and long range correlation $\gamma^2(f_D)$ (c) during the L-I-H transition.

6. Long range correlations

Both the pulsing and GAM are highly correlated spatially. *FIG. 6(e)* shows the γ^2 coherence for f_D (flow - green) and S_D (turbulence-red) fluctuations at the GAM frequency between two Doppler reflectometers probing the same flux surface $\rho_{pol} \approx 0.98$, but in opposite toroidal sectors (sectors 5 & 13) with $\sim 180^\circ$ toroidal separation and different heights (several tens of degrees poloidal separation). The GAM flow peak coherence is around 90% in L-mode, dropping slightly into the I-phase and then recovering towards the H-mode transition - which is not quite achieved in this shot due to insufficient ECRH power. Long-range correlation of low frequency potential / E_r fluctuations are thought to indicate zonal activity and there are several examples of its enhancement during, or prior to, mode transitions [15–17]. In the L-mode phase there is a modest modulation in the density fluctuation envelope at the GAM frequency (pressure side-band mode) which is initially well correlated, but disappears in the I-phase. *FIG. 7(c)* shows the radial profile of the $\gamma^2(f_D)$ GAM flow peak. In this example the sector 5 reflectometer channel is held at the GAM maxmima radial location $\rho_{pol} \approx 0.985$ while the sector 13 channel is scanned radially. For the L-mode phase the GAM is well correlated across the entire GAM zonal ring with a peak coherence of almost 90%. The correlation is independent of the local q value, thus confirming the $m = n = 0$ mode structure of the GAM [2,3]. In the I-phase the correlation weakens (as in *FIG. 6(e)*) and the radial extent narrows, before disappearing completely in the H-mode. The narrowing of the correlation profile on the outboard side follows the erosion of the GAM amplitude zonal width. The pulsing, unlike the GAM, extends right across the plasma edge pedestal region into the near SOL.

7. Power - density dependence

FIG. 8 shows the E_r well minimum vs the H_{98} confinement factor for a range of discharge conditions from ohmic to improved H-modes. Ohmic and NBI heated L-modes have a weak E_r scaling (-4 to -8 kV/m) over a broad confinement span - excepting two borderline ICRH cases. H-modes show a stronger scaling (-20 to -55 kV/m) over similar confinement span. The I-phase sits below the H-mode range forming a continuum. The I-phase also sits below the low density branch of the usual H-mode power threshold, as shown by the blue points in *FIG. 9*. Here the net absorbed power $P_{net} = P_{ohmic} + P_{heat} - dW/dt$ is plotted vs the line averaged core density for a range of ohmic, I-phase and L-mode discharges where GAMs were present. There are no GAMs in the H-mode cases (red points) which resulted from a transition from an I-phase. The shaded bar indicates the H-mode threshold power P_{thr} for recent AUG conditions (grey points: cf. [18]). Observations from many discharges confirm that the L to I-phase is a sharp transition with a well defined threshold while the transition from an I-phase to a clear H-mode appears much softer, cf. *FIG. 3*. Only a few high power L-mode GAMs have been observed at high density - due to strong damping - with rather low frequencies $f_{GAM} < 8$ kHz. So far, no cases of I-phase GAMs have been observed for the high-density P_{thr} branch. With increasing density both the limit-cycle/pulse and the GAM frequency fall (as T_e decreases with increasing density), until at very high collisionality, i.e. densities $\bar{n}_e > 5 \times 10^{19}$ m^{-3}, the transition from L-mode appears to proceed more directly to the H-mode without an intervening I-phase.

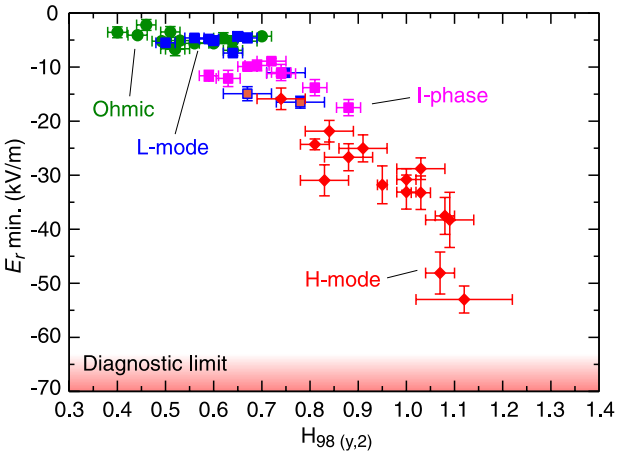

FIG. 8: E_r well depth vs H_{98} energy confinement factor for a range of discharges.

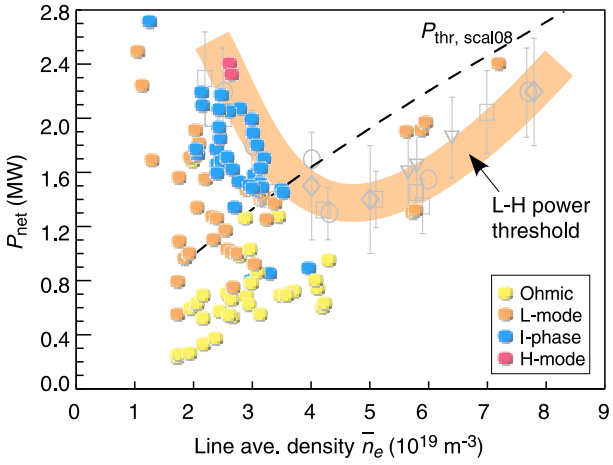

FIG. 9: GAM existence diagram: Net power vs line averaged core density. Shaded bar indicates L-H power threshold.

8. Summary and discussion

In summary, strong domineering GAMs exist in the turbulent, low mean-flow-shear L-mode edge region, but are suppressed in the quiescent, high mean-flow-shear H-mode. Across the L-H transition the GAM - mean equilibrium flow and turbulence display a complex interaction - dependent on the plasma density or collisionality. At low edge densities and high q - where the GAM is strongest - the strong turbulence drive (heating power just below the low density H-mode threshold) creates a low frequency pulsing effect, where a rising turbulence triggers a strong GAM flow oscillation, the shearing of which in-turn suppresses the turbulence and switches-off the GAM, leading to a limit-cycle behaviour. This intermediate limit-cycle

regime supports larger edge pressure gradients and consequently stronger mean-flows and improved energy confinement than a pure L-mode. As the H-mode transition is approached the GAM amplitude and long range coherency initially rise while its zonal radial width is reduced - locally enhancing the velocity shearing - which may well be the trigger for the subsequent mean equilibrium shear feedback loop. Finally, in the fully developed H-mode the coherent GAM oscillation is replaced by large amplitude broad-band flow fluctuations - which may be equally effective in decorrelating turbulent eddies as the higher frequency GAM. With increasing collisionality/density the intermediate regime closes out, coinciding with the switch to the high-density H-mode power threshold branch.

References

[1] DIAMOND, P.H., ITOH, S-I., ITOH, K. and HAHM T.S., "Zonal flows in plasma - a review", Plasma Phys. Control. Fusion **47** (2005) R35.
[2] ITOH, K., et al., "Physics of zonal flows", Phys. Plasmas **13** (2006) 055502.
[3] FUJISAWA, A., "A review of zonal flow experiments", Nucl. Fusion **49** (2009) 013001.
[4] TERRY, P.W., "Suppression of turbulence and transport by sheared flow", Rev. Mod. Phys. **72** (2000) 109.
[5] KIM, E.J. and DIAMOND, P.H., "Zonal flows and transient dynamics of the L-H transition", Phys. Rev. Lett. **90** (2003) 185006.
[6] NAGASHIMA, Y., et al., "Observation of edge Reynolds stress increase preceding an L-H transition in Compact Helical System", Plasma Fusion Res. **5** (2010) 022.
[7] MOYER, R.A., et al., "Increased nonlinear coupling between turbulence and low frequency fluctuations at the L-H transition", Phys. Rev. Lett. **87** (2001) 135001.
[8] MCKEE, G.R., et al., "Dependence of the L to H-mode power threshold on toroidal rotation and the link to edge turbulence dynamics", Nucl. Fusion **49** (2009) 115016.
[9] CONWAY, G.D., et al., "Direct measurement of zonal flows and geodesic acoustic mode oscillations in ASDEX Upgrade using Doppler reflectometry", Plasma Phys. Control. Fusion **47** (2005) 1165.
[10] CONWAY, G.D., et al., "Interaction of mean and oscillating plasma flows across confinement mode transitions", Plasma Fusion Res. **5** (2010) S200* - In press.
[11] CONWAY, G.D., et al., "Amplitude behaviour of geodesic acoustic modes in the ASDEX Upgrade tokamak", Plasma Phys. Control. Fusion **50** (2008) 085005.
[12] ESTRADA, T., et al., "L-H transition experiments in the TJ-II", Proc. 37th EPS Conf. Plasma Phys., Dublin (2010) P1.1027.
[13] ZWEBEN, S.J., et al., "Quiet periods in edge turbulence preceding the L-H transition in NSTX", Phys. Plasma **17** (2010) - In press.
[14] ESTRADA, T., et al., "Sheared flows and transition to improved confinement regime in the TJ-II stellarator", Plasma Phys. Control. Fusion **51** (2009) 124015.
[15] MANZ, P., et al., "Polidal mode structure of long-distance correlation of fluctuations under strong ExB shear in the torsatron TJ-K", Phys. Plasma **16** (2009) 042309.
[16] XU, Y., et al., "Long-distance correlation and zonal flow structures induced by mean ExB shear flows in the biasing H-mode at TEXTOR", Phys. Plasma **16** (2009) 110704.
[17] HIDALGO, C., et al., "Multi-scale physics mechanisms and spontaneous edge transport bifurcations in fusion plasmas", Eur. Phys. Lett. **87** (2009) 55002.
[18] RYTER, F., et al., "H-mode threshold and confinement in helium and deuterium in ASDEX Upgrade", Nucl. Fusion **49** (2009) 062003.